

1        **Near-infrared-triggered synergistic therapy with Ru-based nanocomposite**  
2                    **hydrogel for eradicating multidrug-resistant wound infections**

3                    Zehui Xiao<sup>1</sup>, Bingcong Ji<sup>1</sup>, Jiangli Cao, Ting Du\* and Xinjun Du\*

4 State Key Laboratory of Food Nutrition and Safety, College of Food Science and  
5 Engineering, Tianjin University of Science and Technology, Tianjin 300457, PR China

6

7        **Materials and method**

8        **Synthesis of Ru NPs**

9        First, 0.5 g of cetyltrimethylammonium bromide (CTAB) was weighed and  
10 dissolved in 46 mL of deionized water. The solution was stirred at room temperature  
11 for 2 h, after which 12.9 mg of NaOH was gradually added. The mixture was then  
12 heated to 80 °C under continuous stirring. Subsequently, 32.6 mg of RuCl<sub>3</sub> was  
13 weighed, dissolved in deionized water, and slowly introduced into the aforementioned  
14 solution. The reaction was allowed to proceed at 80°C for 2 h. Then, 1.0 mL NaBH<sub>4</sub>  
15 (1.0 M) was added dropwise to the mixture. After an additional 2 h of stirring, the  
16 reaction solution was centrifuged and sequentially washed with acetone, hydrochloric  
17 acid, ethanol, and deionized water. Finally, the obtained product was dried under  
18 vacuum and designated as Ru NPs.

19        **Synthesis of BBR@Ru NPs-PEI**

20        The Ru NPs synthesized previously were dispersed in methanol. Berberine (BBR)  
21 was then added at a concentration ratio of 1:3 (Ru NPs: BBR) and dissolved via  
22 ultrasonication. The mixture was stirred at room temperature for 24 h to ensure the

23 loading of BBR onto the Ru NPs. Upon completion of the reaction, the product was  
24 isolated by centrifugation and sequentially washed with methanol and deionized water  
25 to obtain the BBR@Ru NPs.

26 Subsequently, polyethyleneimine (PEI) solution (5.0 mg/mL) was added to the  
27 suspension of BBR@Ru NPs. The mixture was stirred and subjected to ultrasonication  
28 for 2 h to achieve uniform dispersion. Finally, the resulting product was collected by  
29 centrifugation, washed thoroughly with deionized water, and dried under vacuum to  
30 yield the BBR@Ru NPs-PEI.

### 31 **Synthesis of BBR@Ru NPs-PEI hydrogel (RBP hydrogel)**

32 Briefly, 0.5 g of carboxymethyl chitosan (CMCS) was dissolved in 10 mL of  
33 deionized water. Subsequently, 1-ethyl-3-(3-dimethylaminopropyl) carbodiimide  
34 hydrochloride (EDC) and N-hydroxysuccinimide (NHS) solutions were added  
35 sequentially to the CMCS solution. The BBR@Ru NPs-PEI was then introduced into  
36 the mixture and stirred thoroughly to ensure homogeneity. The reaction was allowed to  
37 proceed at room temperature for 30 min, resulting in the formation of the BBR@Ru  
38 NPs-PEI hydrogel (RBP hydrogel).

### 39 **Analysis of RBP hydrogel photothermal property and photostability**

40 Briefly, RBP hydrogels at varying concentrations (30  $\mu\text{g/mL}$ , 60  $\mu\text{g/mL}$ , 120  
41  $\mu\text{g/mL}$ ) were exposed to 808 nm NIR light at different power densities (0.5  $\text{W/cm}^2$ , 1.0  
42  $\text{W/cm}^2$ , and 1.5  $\text{W/cm}^2$ ) for 5 min. The temperature changes during this period were  
43 recorded to evaluate the photothermal performance. Additionally, the photothermal  
44 stability of the RBP hydrogel was investigated by subjecting it to 10 on-off cycles of

45 808 nm laser irradiation.

46 For the measurements of photothermal conversion efficiency, the RBP hydrogel  
47 aqueous solution (120 µg/mL) was irradiated by 808 nm laser. The temperature changes  
48 of the solution within 5 min were recorded by Fluke infrared thermal imager (recorded  
49 once every 60 s). The photothermal conversion efficiency ( $\eta$ ) was calculated by  
50 Equation (1).

$$\eta = \frac{hA(T_{max} - T_{surr}) - Q_{dis}}{I(1 - 10^{-A\lambda})} \quad (1)$$

52  $T_{surr}$  and  $T_{max}$  respectively represent the ambient temperature and the equilibrium  
53 temperature that RBP hydrogel can reach after being irradiated by laser.  $A\lambda$  indicates  
54 the absorbance of RBP hydrogel at 808 nm.  $I$  represents the laser power, and  $Q_{dis}$   
55 indicates the heat loss. Therefore, in Equation (1), only  $hA$  is unknown. Subsequently,  
56 we calculate  $hA$  using Equations (2) and (3).

$$\theta = \frac{T - T_{surr}}{T_{max} - T_{surr}} \quad (2)$$

$$\tau = \frac{m_p c_p}{hA} \quad (3)$$

59  $\theta$ ,  $\tau$ ,  $c_p$  and  $m_p$  are dimensionless constants, the time constant of the sample, the  
60 specific heat capacity of water, and the mass of the RBP hydrogel solution respectively.  
61 Through Equation (4), we can calculate the time constant ( $\tau$ ).

$$\tau = \frac{t}{-\ln(\theta)} \quad (4)$$

63 Based on the above equation, the photothermal conversion efficiency (PCE) of  
64 RBP hydrogel can be calculated.

### 65 ***In vitro* antibacterial activity of RBP hydrogel**

66 The *in vitro* antibacterial activity of the RBP hydrogel against Methicillin-resistant  
67 *Staphylococcus aureus* (MRSA) and *Pseudomonas aeruginosa* (*P. aeruginosa*) was  
68 evaluated using the coating plate method. Briefly, bacterial suspensions were incubated  
69 with RBP hydrogels at varying concentrations (30, 60, and 120 µg/mL) for 1 h, with  
70 sterile PBS solution serving as the control. For the illumination group, the samples were  
71 irradiated with an 808 nm laser (1.0 W/cm<sup>2</sup>) for 5 min. Subsequently, 50 µL from each  
72 reaction solution was spread onto LB agar plates. After overnight incubation at 37°C,  
73 the colonies on each plate were counted to determine bacterial survival rates..

74 To further assess bacterial viability, the bacterial solutions were stained with  
75 propidium iodide (PI) and 4',6-diamidino-2-phenylindole (DAPI) for live/dead  
76 staining, while ROS levels were detected using 2',7'-dichlorodihydrofluorescein  
77 diacetate (DCFH-DA). Additionally, the protein content of each group was quantified  
78 using a BCA protein concentration assay kit (Jiancheng Biotechnology Co., Nanjing,  
79 China), and nucleic acid content was measured using a DNA and RNA assay kit  
80 (TIANGEN BIOTECH, Beijing).

### 81 ***In vitro* biofilm removal assays**

82 MRSA and *P. aeruginosa* (OD 0.6-0.8) were inoculated into a 96-well plate and  
83 cultured at 37°C for 48 h to allow biofilm formation. The biofilms were treated with  
84 RBP hydrogel, either with or without NIR irradiation (808 nm, 1.0 W/cm<sup>2</sup>, 10 min).  
85 After treatment, the supernatant was removed and the biofilms were fixed with 99%  
86 methanol for 15 min. Subsequently, they were stained with 0.2% crystal violet for 30

87 min. After washing three times with PBS to remove unbound dye, the crystal violet  
88 retained by the biofilm was dissolved in ethanol. The absorbance of the eluted dye was  
89 measured at 570 nm to quantify the residual biofilm biomass.

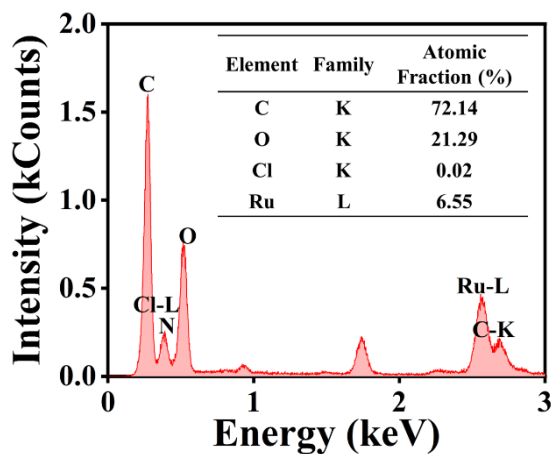
90 Additionally, the treated biofilms were visualized using laser confocal  
91 microscopy. Briefly, biofilms subjected to different treatments were fixed with 4%  
92 glutaraldehyde overnight. After discarding the supernatant and washing with PBS, the  
93 biofilms were stained with SYBR Green I for 30 min in the dark. The biofilm  
94 morphology of each group was then observed using confocal laser scanning microscopy  
95 (Leica TCS SP8).

96 To further investigate the effects of the treatments, total RNA was extracted from  
97 bacteria following different experimental conditions. The relative expression levels of  
98 virulence factors were analyzed by reverse transcription quantitative polymerase chain  
99 reaction (RT-qPCR) using the primers listed in Table S1.

#### 100 ***In vivo* wound healing experiment**

101 A mouse wound model of MRSA infection was established to evaluate the *in vivo*  
102 antibacterial efficacy of the RBP hydrogel. Under sterile conditions, a wound with a  
103 diameter of approximately 8.0 mm was created on the dorsal skin of BALB/c mice (6–8  
104 weeks old, 18–22 g, female). Subsequently, 100  $\mu$ L of MRSA suspension ( $10^7$   
105 CFU/mL) was subcutaneously injected into the wound site and allowed to incubate for  
106 24 h. The mice were then randomly divided into four groups: PBS-NIR<sub>(+)</sub>, PBS-NIR<sub>(-)</sub>,  
107 RBP hydrogel-NIR<sub>(-)</sub>, RBP hydrogel-NIR<sub>(+)</sub>. The NIR irradiation groups were exposed  
108 to an 808 nm laser (1.0 W/cm<sup>2</sup>) for 30 s.

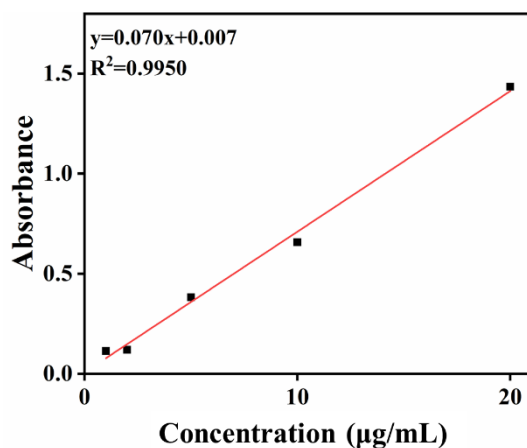
109 On days 0, 1, 3, 5, 7, and 9 of treatment, wound areas were photographed and the  
110 body weights of the mice were recorded. Bacterial colonies from the wound sites were  
111 collected, smeared, and quantified to assess bacterial load. On day 9, all mice were  
112 euthanized, and tissues from the heart, liver, spleen, lung, kidney, and epithelial regions  
113 were harvested for hematoxylin and eosin (H&E) staining and Masson's trichrome  
114 staining to evaluate tissue morphology and collagen deposition. Additionally, blood  
115 samples were also collected for biochemical analysis. All the animal tests were  
116 approved by the animal care and experiment committee of Tianjin University of  
117 Science & Technology.



119

120

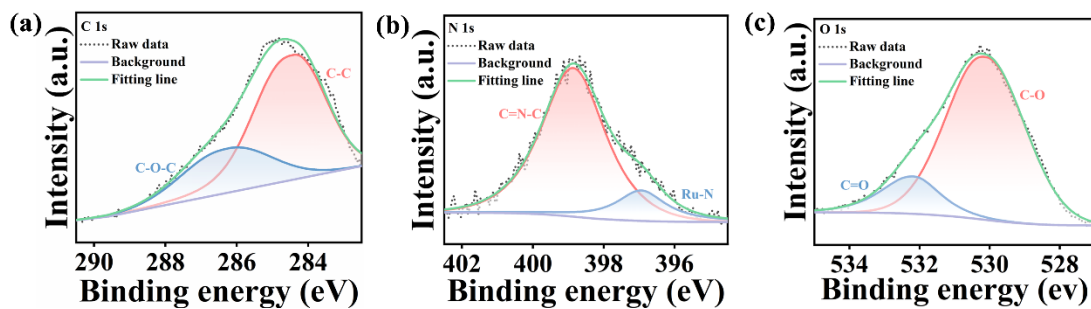
Fig. S1. EDS analysis of BBR@Ru NPs-PEI.



121

122

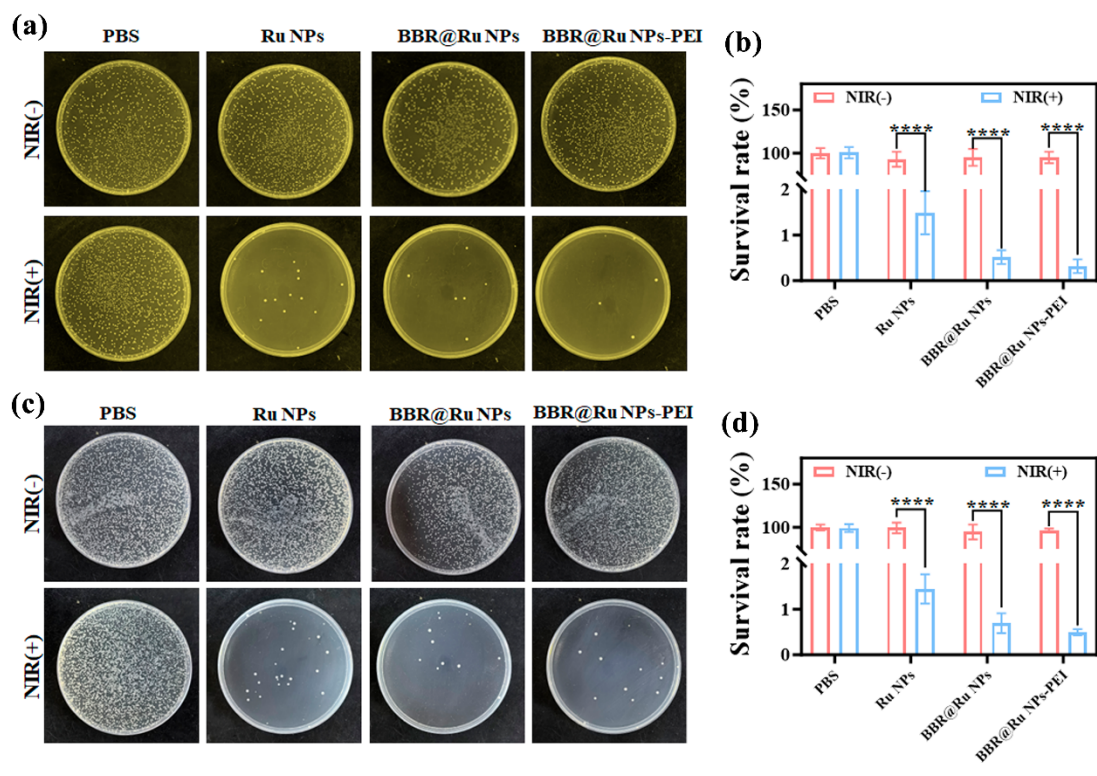
Fig. S2. The UV-Vis absorption of BBR at different concentrations.



123

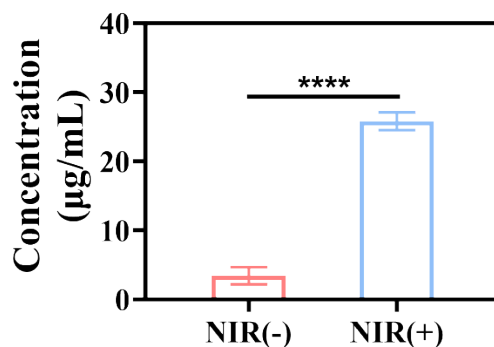
124

Fig. S3. High-resolution XPS spectra of C 1s (a), N 1s (b) and O 1s (c) orbitals.



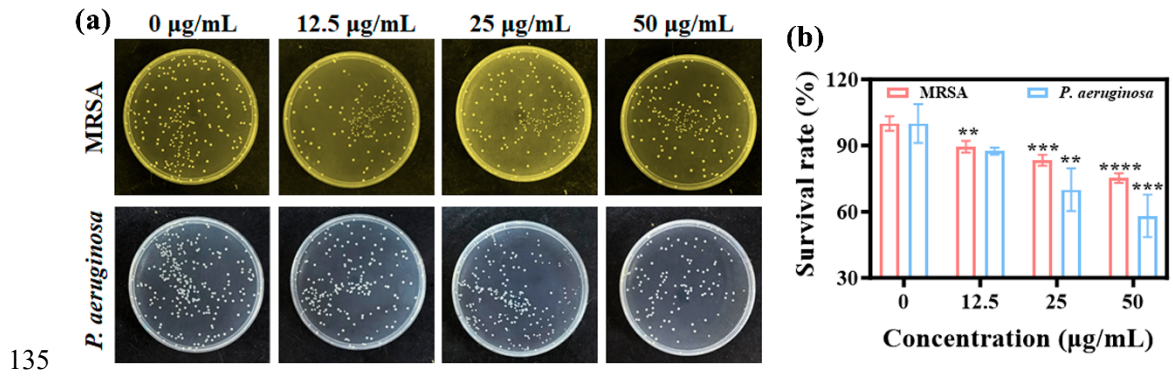
125

126 **Fig. S4.** MRSA (a) and *P. aeruginosa* (c) colony images after treatment with Ru NPs,  
 127 BBR@Ru NPs or BBR@Ru NPs-PEI (120 µg/mL). The survival rate of MRSA (b) and  
 128 *P. aeruginosa* (d) (n=3). Error bars represent means ± SD. Differences between groups  
 129 were tested using one-way ANOVA followed by Tukey's multiple comparisons test.  
 130 \*\*\*\*p < 0.0001.

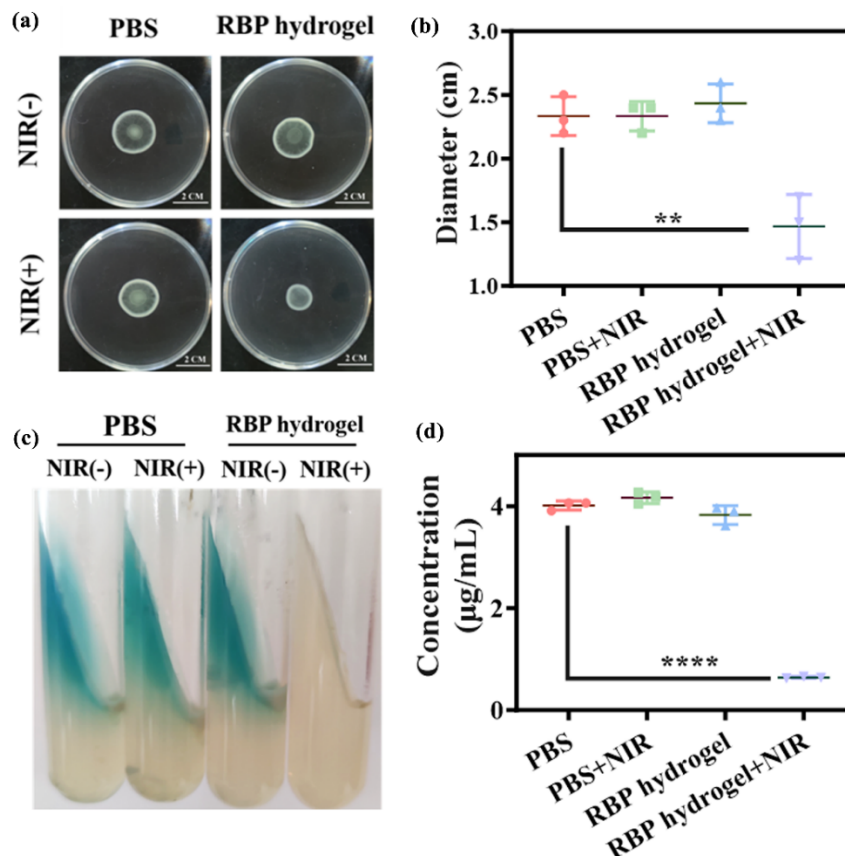


131

132 **Fig. S5.** Determination of BBR Release (n=3). Error bars represent means ± SD.  
 133 Differences between groups were tested using one-way ANOVA followed by Tukey's  
 134 multiple comparisons test. \*\*\*\*p < 0.0001.

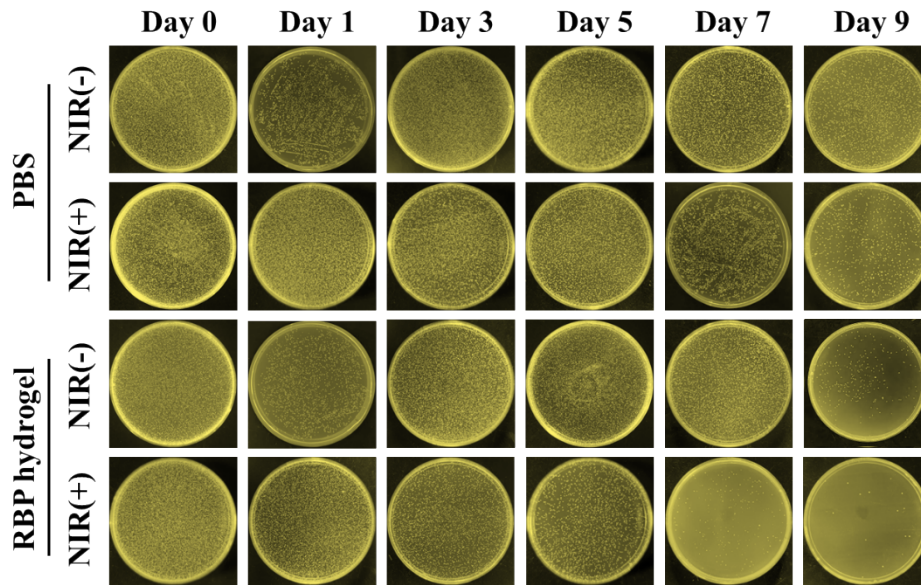


135  
 136 **Fig. S6.** (a) MRSA and *P. aeruginosa* colony images after treatment with BBR at  
 137 different concentrations (0-50 µg/mL). (b) The survival rate of MRSA and *P.*  
 138 *aeruginosa* (n=3). Error bars represent means ± SD. Differences between groups were  
 139 tested using one-way ANOVA followed by Tukey's multiple comparisons test. \*\*p <  
 140 0.01, \*\*\*p < 0.001, \*\*\*\*p < 0.0001.



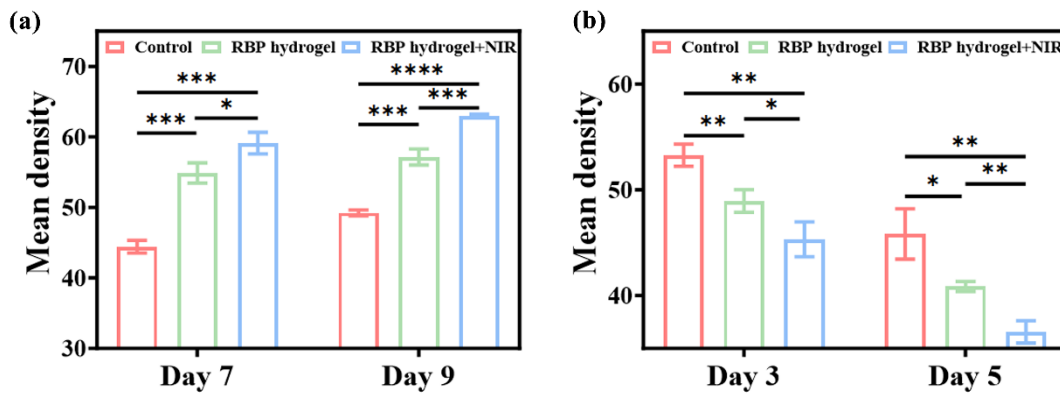
141  
 142 **Fig. S7.** (a) Swarming motility and (b) corresponding colony diameters of *P.*  
 143 *aeruginosa* following different treatments (n=3). Pyocyanin secretion (c) and its

144 corresponding quantification (d) following different treatments (n=3). Error bars  
 145 represent means  $\pm$  SD. Differences between groups were tested using one-way ANOVA  
 146 followed by Tukey's multiple comparisons test. \*\*p < 0.01, \*\*\*\*p < 0.0001.



147

148 **Fig. S8.** Bacterial colonization in wound of mice after different treatments.



149

150 **Fig. S9.** Quantification of IL-6 (a) and VEGF (b) fluorescence intensity (n=3). Error  
 151 bars represent means  $\pm$  SD. Differences between groups were tested using one-way  
 152 ANOVA followed by Tukey's multiple comparisons test. \*p < 0.05, \*\*p < 0.01, \*\*\*p  
 153 < 0.001, \*\*\*\*p < 0.0001.